

# Wake Vortex Measurements of an Ogive Cylinder at $\alpha = 36$ Degrees

F.K. Owen\*  
Palo Alto, Calif.

and

D. A. Johnson†  
NASA Ames Research Center, Moffett Field, Calif.

Three-dimensional laser velocimeter measurements have been made of the wake vortices of a slender tangent-ogive body which had nose and body fineness ratios of 3.5 and 12, respectively. Data were obtained at an angle of attack of 36 deg, a freestream Mach number of 0.6, and a Reynolds number based upon body diameter of 170,000. Details of the mean flowfield are presented, and features of the turbulent and unsteady nature of the vortex flowfield are discussed. Problems associated with obtaining meaningful vortex measurements in high-speed flows are addressed.

## Introduction

ASYMMETRIC vortex flows are known to produce large side forces and yawing moments on bodies of revolution, although the mechanisms through which these occur are not well understood. Unfortunately, the documentation of asymmetric forebody flowfields is difficult, since the degree or even the direction of the asymmetry can be influenced by extremely small changes in nose shape or body roll.<sup>1,2</sup> Flow turbulence may also effect the overall steadiness of the flowfield. Lamont and Hunt<sup>3</sup> have shown that freestream turbulence can cause switching of the vortex flow patterns. Such time-dependent flowfield behavior is difficult to document unless conditional sampling techniques are used (see Ref. 4). Despite these experimental difficulties detailed information has been obtained primarily using pitot probes.<sup>1</sup> However, since wake flows can be sensitive to local geometry and probe interference and since streamline curvature and associated static pressure variations could compromise pitot or hot-wire measurements, it is desirable to pursue nonintrusive measurement techniques. Direct comparison between laser vapor screen and pitot measurements of vortex core location<sup>5</sup> have shown that flowfield probes can cause vortex displacement. Problems associated with turbulent structure measurements are even more acute since linearized hot-wire data interpretations are not accurate in highly turbulent wake flows. The laser velocimeter with its nonintrusive applicability to highly turbulent flows appears to be a more appropriate instrument for the documentation of vortex flowfields. Since the documentation of asymmetric vortex flows can present additional and unwanted experimental complications, steady symmetric vortex flows provide a logical first step in assessing the capabilities of the laser velocimeter for three-dimensional vortex measurements. Although limited measurements have been obtained at low speeds,<sup>6,7</sup> no turbulence data or high-speed measurements are available. It was with these shortcomings in mind that the present study was undertaken.

## Experimental Details

Tests were conducted in the Ames 2- by 2-ft Transonic Wind Tunnel at a freestream Mach number of 0.6 and unit Reynolds number of 2 million/ft. Wake vortex measurements were obtained for a 1-in. cylindrical afterbody tangent ogive which had a nose fineness ratio of 3.5 and a total or body fineness ratio of 12:1. Flowfield measurements were obtained at two axial stations (Fig. 1) at an angle of attack of 36 deg.

The model was instrumented with constant temperature surface hot film gages of the type used in Ref. 8. Their dynamic response ( $>60$  kHz with negligible phase distortion) was sufficient to determine dynamic characteristics of the vortex shedding. The velocity field in the wake was measured with a two-color forward scatter frequency offset laser velocimeter. This system enabled two velocity components, perpendicular to the optical axis, to be measured simultaneously. However, since the problem is three-dimensional, two sets of measurements are required. During the first set, the laser beams were normal to the tunnel axis so that the axial  $u$  and vertical  $w$  velocity components in tunnel coordinates were measured. These two components were used to determine the vertical velocity in the crossflow plane shown in Fig. 1. For the second set, the transmitting optics were rotated 30 deg about the  $z$  axis and measurements retaken. In this

$\theta_c = 16$  deg TANGENT-OGIVE CYLINDER AT INCIDENCE

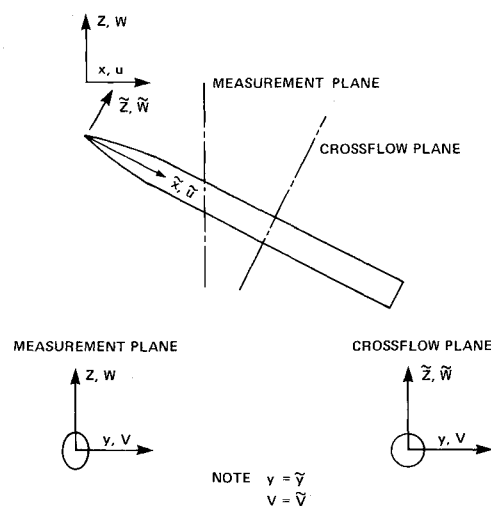


Fig. 1 Coordinate system.

Presented as Paper 78-23 at the AIAA 16th Aerospace Sciences Meeting, Huntsville, Ala., Jan. 16-18, 1978; submitted April 3, 1978; revision received Feb. 8, 1979. This paper is declared a work of the U.S. Government and therefore is in the public domain. Reprints of this article may be ordered from AIAA Special Publications, 1290 Avenue of the Americas, New York, N.Y. 10019. Order by Article No. at top of page. Member price \$2.00 each, nonmember, \$3.00 each. Remittance must accompany order.

Index category: LV/M Aerodynamics.

\*Consultant, P. O. Box 1697. Member AIAA.

†Research Scientist. Member AIAA.

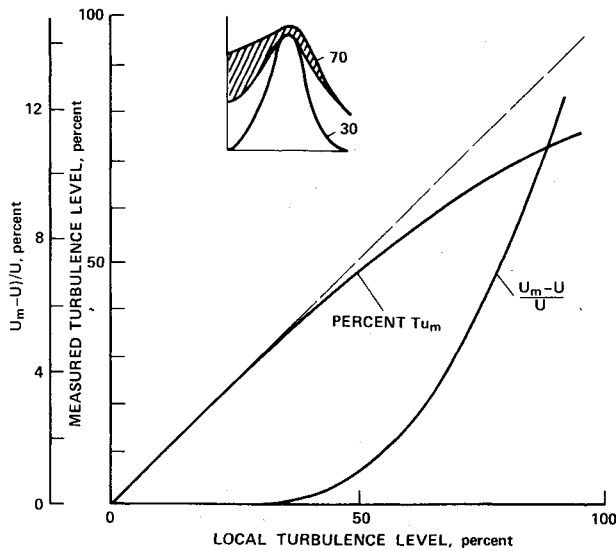


Fig. 2 Errors in the measured mean and rms velocity due to directional ambiguity.

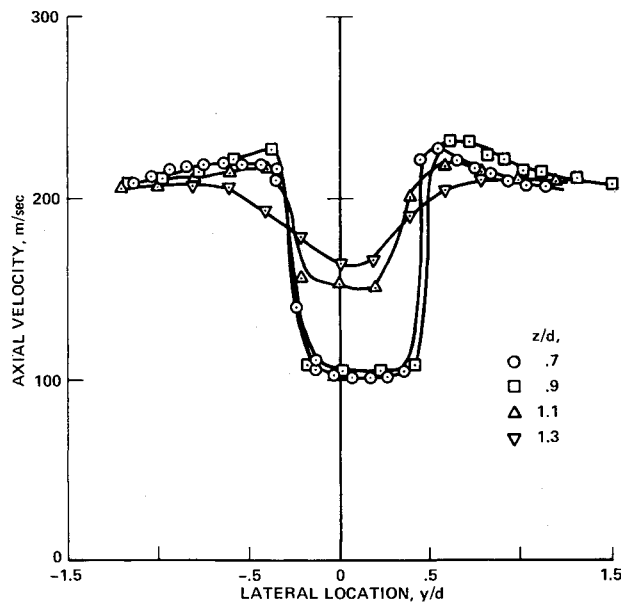


Fig. 3 Mean axial velocity profiles ( $x/d = 4$ ) in wind-tunnel coordinates.

latter case, one component measured was again the vertical velocity whereas the second was a combination of the axial velocity  $u$  and the lateral velocity  $v$  in wind-tunnel coordinates. Since the axial velocity had already been directly measured, the lateral velocity could be calculated. Thus the lateral velocity in the crossflow plane is obtained, since it is the same as that in wind-tunnel coordinates.

Bragg cells, which produced zero-velocity frequency offsets in both color systems, were incorporated to remove directional ambiguity from the measurements. Lack of this capability leads to data interpretation errors in highly turbulent and/or unsteady flows. This problem is illustrated in the insert of Fig. 2, where Gaussian probability density distributions of the instantaneous velocities corresponding to local turbulent intensities of 30 and 70% are presented. With directional ambiguity, negative velocities are assigned their equivalent positive values, which leads to errors in the calculated mean value and standard deviation. The resultant errors are seen to rise sharply for local turbulence intensities above 40%. Thus, it is evident that previous vortex measurements obtained without zero-velocity frequency offset could be subject to significant errors.

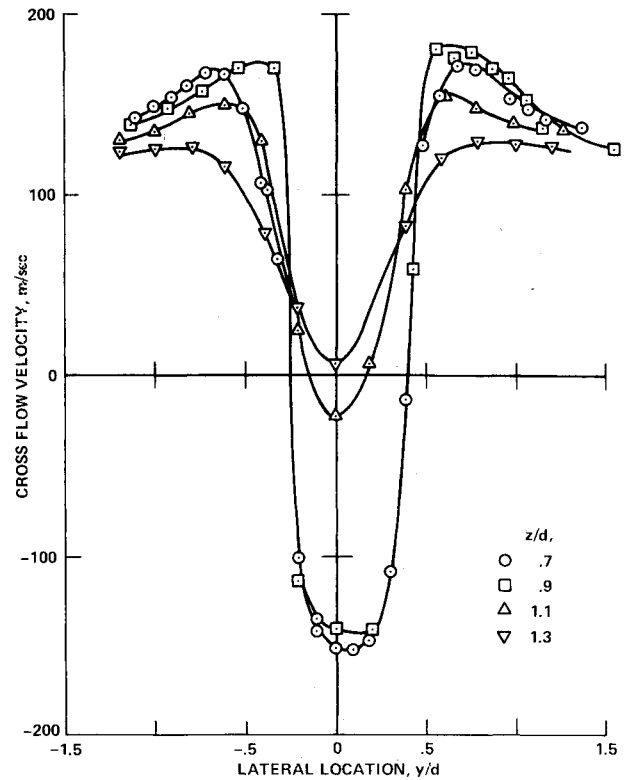


Fig. 4 Mean vertical velocity in crossflow plane ( $x/d = 4$ ).

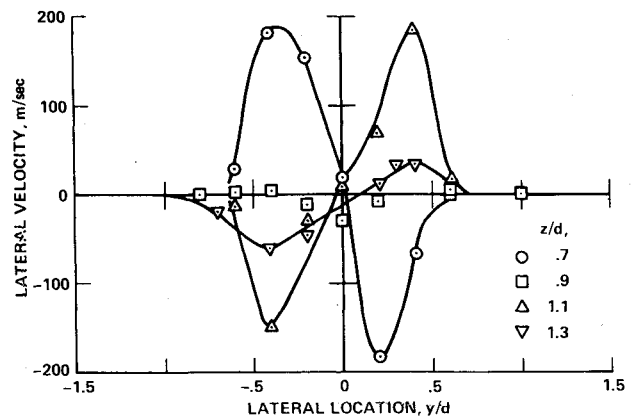


Fig. 5 Mean lateral velocity in crossflow plane ( $x/d = 4$ ).

Maximum optical-system sensitivity is also essential for meaningful vortex measurements since there is always the possibility that only the velocities of larger particles, which have been centrifuged from the vortex, will be observed. This could result in errors in the vorticity measurements and difficulty in obtaining data in the vortex cores. Preliminary laboratory measurements using simultaneous forward- and back-scatter arrangements were carried out on particles of the size distribution used in the symmetric vortex studies.

These measurements stressed the value of a forward-scatter optical system since data rates at least an order of magnitude higher than those in the back-scatter mode were achieved. Previous vortex measurements at low speeds<sup>6,7</sup> both utilized back-scatter systems which, with normal laser power, would probably not be adequate at transonic speeds where problems due to particle lag require the use of smaller particles and hence decreased scattered light intensity. Thus, rather than relying on natural wind-tunnel aerosols for the light scattering, an artificial aerosol of Dioctylphthalate of known size distribution was injected into the wind-tunnel stagnation

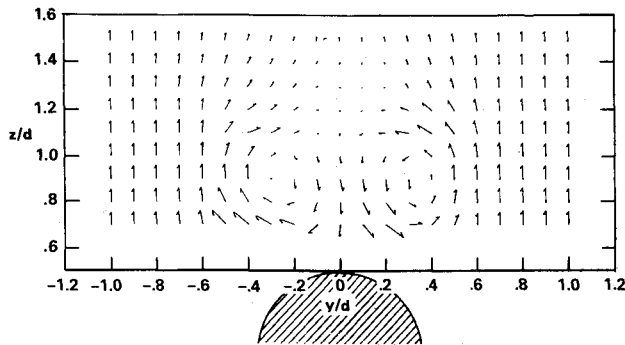


Fig. 6 Velocity vectors ( $x/d = 4$ ).

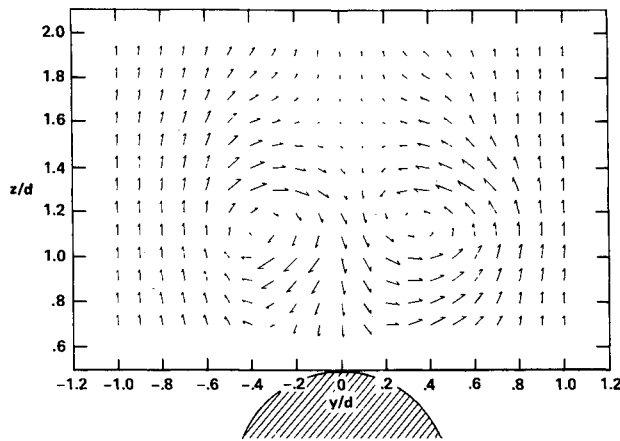


Fig. 7 Velocity vectors ( $x/d = 6$ ).

chamber. This aerosol with a count mean diameter of  $0.7 \mu\text{m}$ , less than one half that of the aerosol used in Ref. 7, provided adequate tracking of the vortex flowfield. To confirm this, axial and vertical measurements were obtained at variable threshold settings on the processing electronics. At high settings, only a few of the larger particles which passed through the center of the probe volume were considered, whereas at low threshold settings velocities of the submicron particles dominated. On the wake centerline at  $y/d = 0.7$ , the mean flow angle varied less than 3 deg even with threshold setting changes which reduced the velocity data rate from 16,000/s to 1000/s. At  $y/d = 1.0$ , a change from 36,000/s to 300/s produced no significant change in the local mean flow angle.

## Discussion

### Mean Flowfield Measurements

As mentioned previously, the laser velocimeter measurements were made in a system of wind-tunnel coordinates. These components were then transformed into the model coordinate system to obtain the vertical and transverse velocities in the crossflow plane. Some of the measurements of the leeward flowfield, 4 diam from the nose, are shown in Figs. 3-5. Figure 3, in which some axial velocity distributions are presented, shows significant overshoots close to the body ( $u/u_\infty \approx 1.2$ ), high mean gradients which occur across the feeding sheets, and a large deficit in the wake. These wake deficits and mean gradients measured close to the body are both much larger than those measured previously at low speeds.<sup>6,7</sup> However, both these features decay quite rapidly, an indication of energetic turbulent motions in the wake.

The maximum vertical velocities ( $w$ ) in the crossflow plane shown in Fig. 4 approach the freestream tunnel velocity and have the form expected of two symmetric-free vortices, except near the wake centerline where vortex interaction appears to dominate. These data are similar to those obtained at low

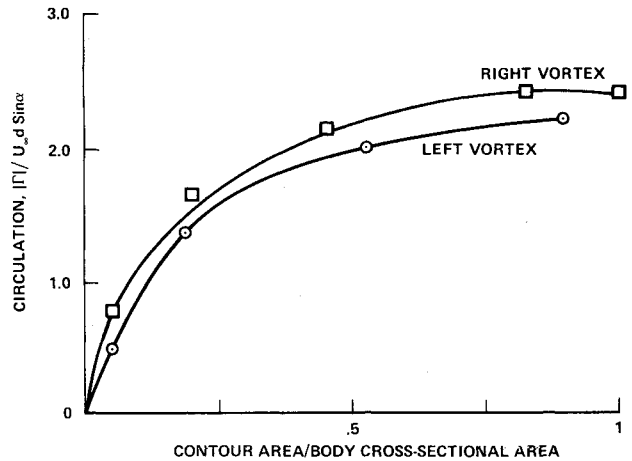


Fig. 8 Variation of circulation with contour area ( $x/d = 4$ ).

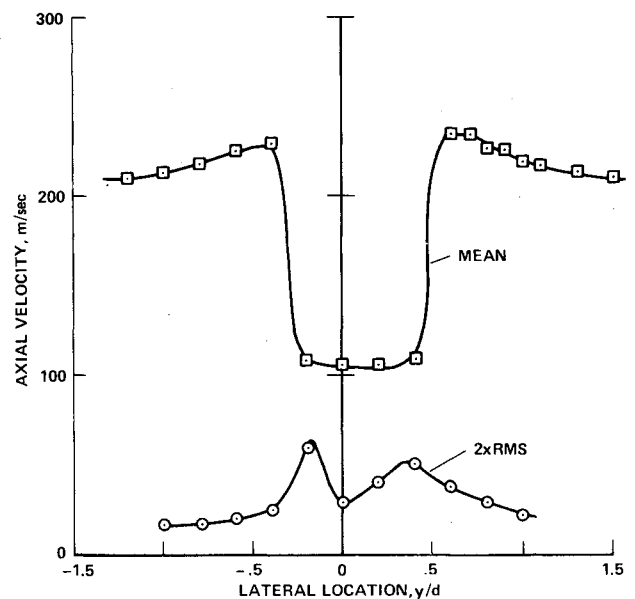


Fig. 9 Mean and rms axial velocity profiles ( $x/d = 4$ ,  $z/d = 0.9$ ).

speeds, although the free vortex form is much more pronounced than in the data of Ref. 6. Lateral crossflow velocities  $\bar{v}$  obtained from measurements normal and 30 deg to the tunnel axis are shown in Fig. 5. These data taken above and below the vortex centers show that again the mean flow gradients are extremely high except in the regions near the vortex cores and that crossflow velocities approaching freestream values are present in the wake. These data, and others obtained throughout the wake at  $x/d = 4$  and 6 stations, have been used to construct the crossflow velocity vector fields which are presented in Figs. 6 and 7.

The circulations of the vortices were found by integrating the crossflow velocity around rectangular contours containing each vortex core. The area of each rectangle was increased in a systematic manner until the contour integral ceased to increase, indicating that all the vorticity had been contained within the contours. It can be seen that, at the  $x/d = 4$  station (Fig. 8), the area that encloses most of the vorticity is approximately equal to the body cross-sectional area. Thus it is apparent that considerable vorticity diffusion had occurred. Similar results were obtained for the  $x/d = 6$  station, although the average vortex strength was higher ( $\approx 3.1$ ) as expected. These vortex strengths are in good agreement with the correlation of Ref. 1.

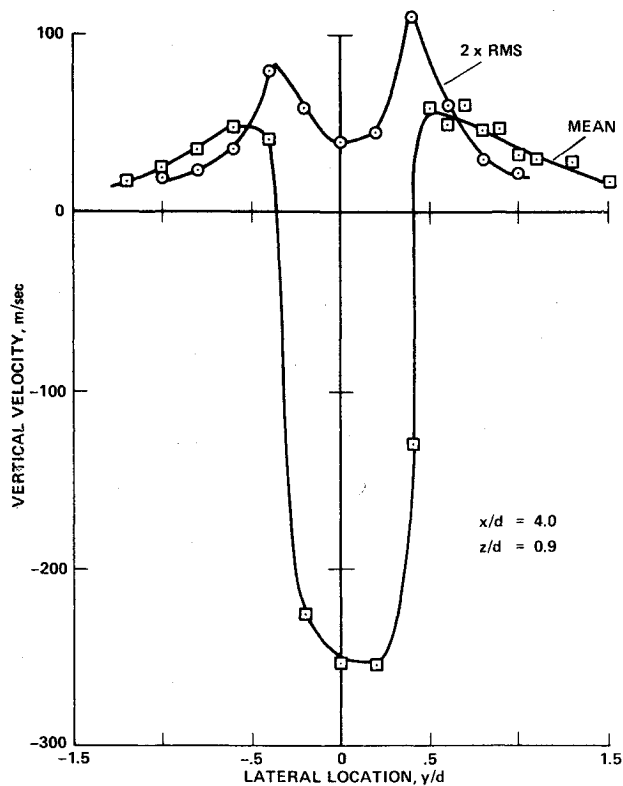


Fig. 10 Mean and rms vertical velocity profile ( $x/d = 4$ ,  $z/d = 0.9$ ).

#### Turbulence Measurements

Some insight into the turbulent and unsteady nature of the vortex flowfield has also been obtained from the laser velocimeter and surface hot-film gage measurements. Consider first the mean and rms velocity profiles across the wake at  $x/d = 6$ . These data (Figs. 9 and 10), obtained at  $z/d = 0.9$ , clearly show double peaks in the rms velocity, one on each side of the wake centerline close to the regions of maximum mean velocity gradient. However, there are also significant rms fluctuation levels in regions of small and zero mean velocity gradient, indicating that larger scale turbulent or unsteady motions are present. These large-scale motions are readily apparent in the surface gage cross-correlation measurements presented in Fig. 11. Toward the stagnation point (Fig. 11a), a clearly defined frequency is evident with an optimum correlation displaced from zero corresponding to vortex convection around the body. In addition, there is little decay in the correlation over many cycles, indicating that both gages are seeing the same disturbances. However, on the leeside of the body the optimum correlation is greatly reduced and decays at a much faster rate, indicating that the two gages are not always responding to the same vortex. Since their circumferential spacing is only 30 deg, this indicates that there may be substantial vortex motions. Such motions give rise to large rms velocity fluctuations, particularly in the vertical velocity component (see Fig. 10). Indeed, in the regions of the time-averaged velocity zeros ( $y/d = \pm 0.4$ ), bimodal velocity probability density distributions were observed, as can be seen for example, in Fig. 12. Such distributions show that a bistable velocity field exists in parts of the flowfield and that vortex movement may be present. These results at a nondimensional, impulsively started cylinder time parameter  $\bar{t} = x/r \tan \alpha = 8.7$  show a preferred state which is disturbed on occasions and is in substantial agreement with the observations of Ref. 3. At  $\bar{t} = 8.1$ , an analysis of the pressure difference traces presented in Ref. 3 would show similar bimodal probability density distributions. These observations suggest that there could be a region of incipient asymmetric vortex shedding, i.e., unsteady vortex motions

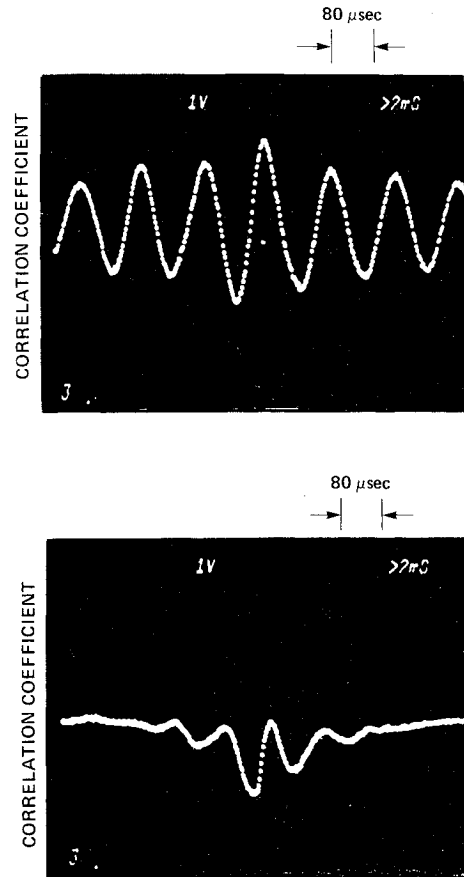


Fig. 11 Surface hot-film cross-correlation measurements.

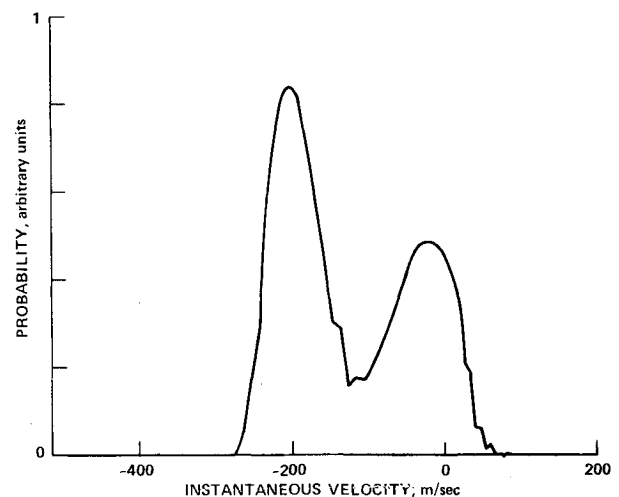


Fig. 12 Vertical velocity probability density function.

induced by vortex interaction. This mechanism has been observed to precede the establishment of relatively steady vortex asymmetry.

As would be expected from the cross-correlation measurements, surface hot-film spectra in the windward flowfield also show a clear energy peak at a frequency of 1250 Hz. If this frequency is introduced into the calculation of a crossflow Strouhal number ( $S = nd/U_\infty \sin \alpha \approx 0.2$ ), excellent agreement is found with Morkovin's<sup>9</sup> two-dimensional cylinder correlation. Since the thin film gage oscillations are related to vortex movement in the wake,<sup>4</sup> these results suggest that incipient asymmetric vortex interactions may be locked to a Strouhal shedding frequency.

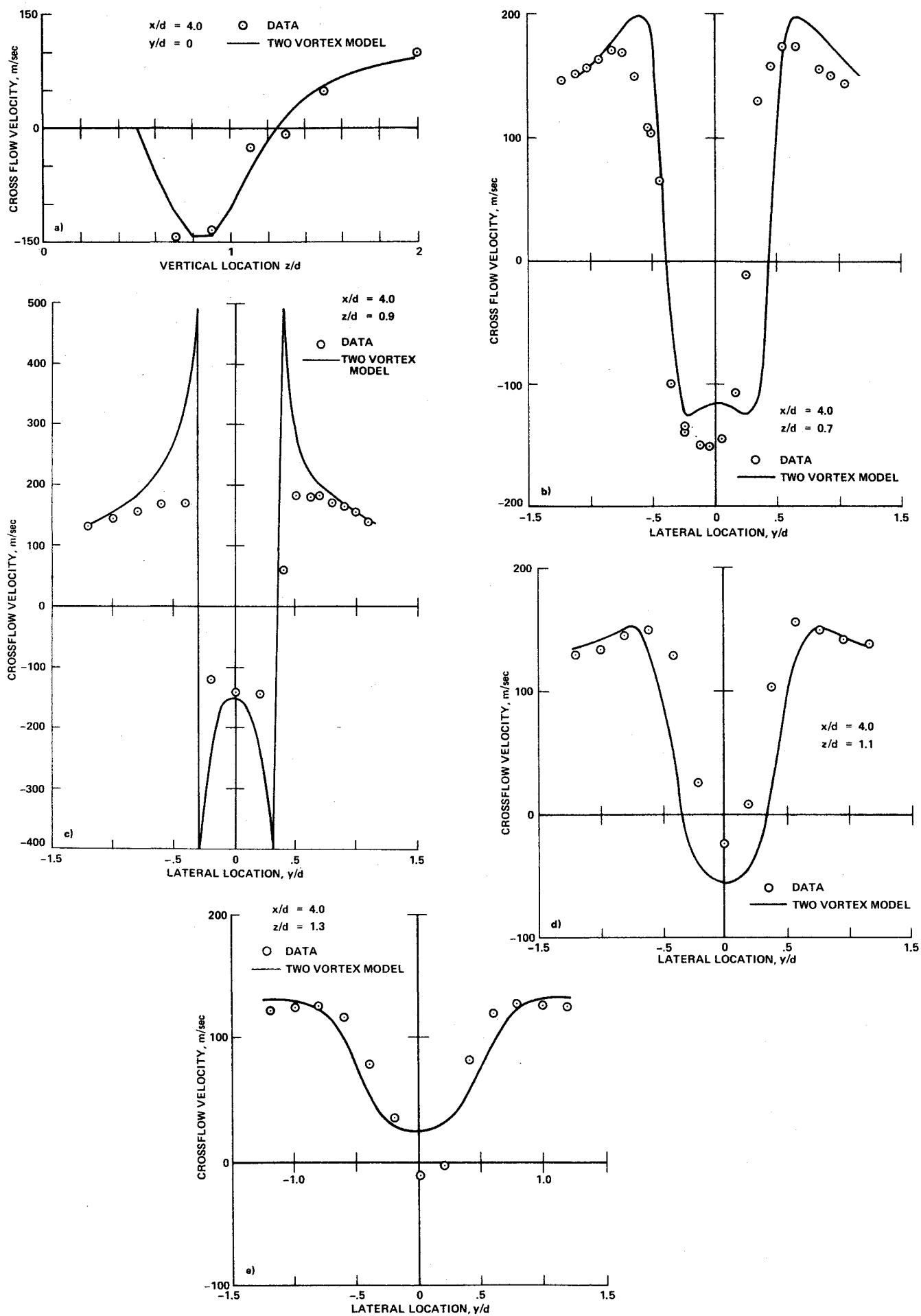


Fig. 13 Comparison of experimental and predicted vertical crossflow velocities ( $x/d = 4$ ).

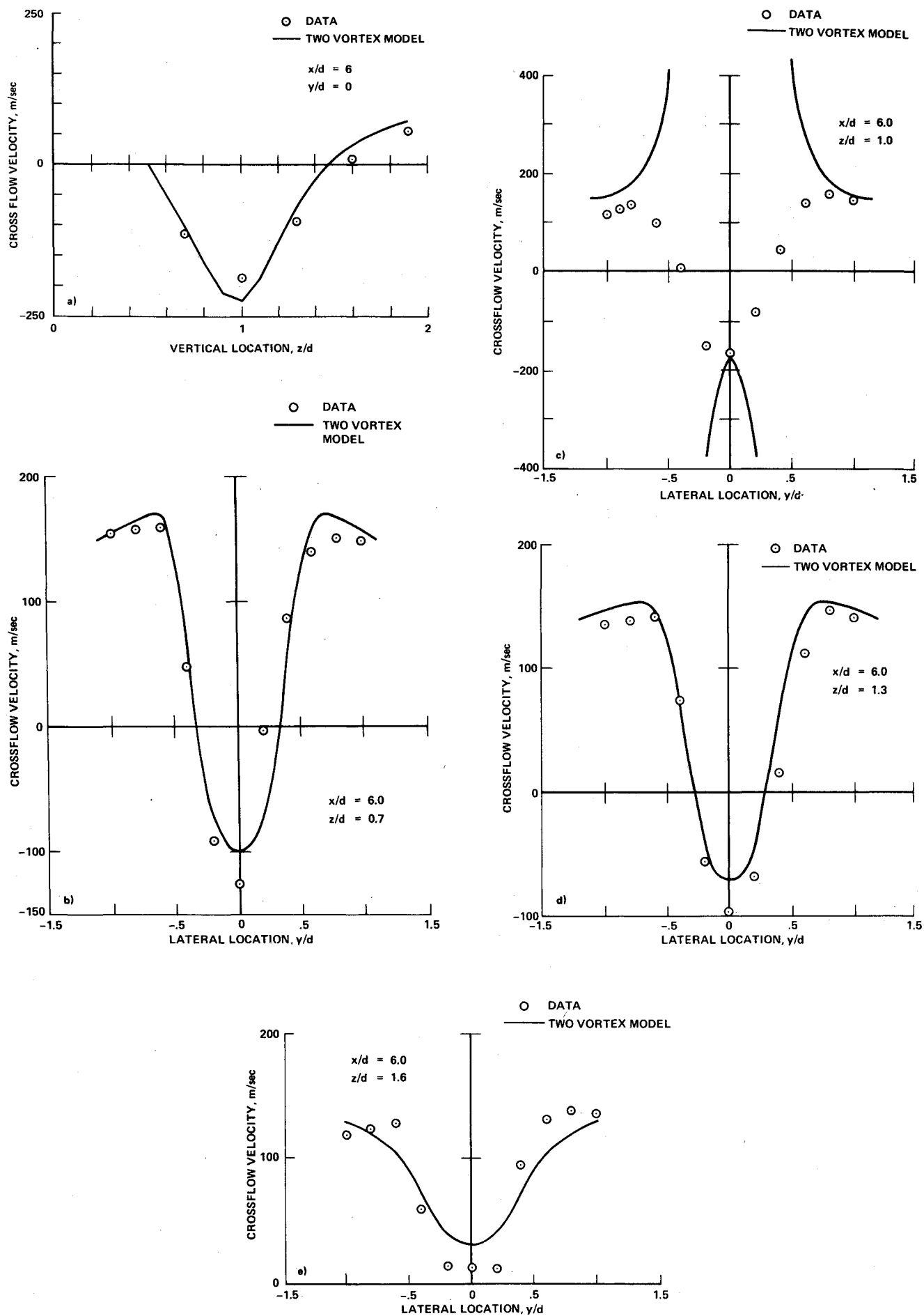


Fig. 14 Comparison of experimental and predicted vertical crossflow velocities ( $x/d = 6$ ).

### Flowfield Modeling

In lieu of a reliable Navier-Stokes predictive scheme at transonic speeds, the flowfield data have been compared with classical two-dimensional theory. Following Nielsen,<sup>10</sup> we consider two vortices in the presence of a circular cylinder in which the vorticity generated in the viscous layer ahead of separation moves along the feeding sheets into the two cores. Since the measured vertical and axial velocity profiles were so symmetric at each station, we have assumed identical positions and absolute vortex strengths. The values used were straightforward arithmetic averages of the two vortex properties at each station. With these assumptions, we may calculate the resulting crossflow velocities by

$$\bar{v} + i\bar{w} = -iU_{\infty} \sin\alpha(1 + d^2/4\xi^2) - 1/2\pi \sum_{j=1}^N \Gamma_j [1/(\xi - \xi_j) - 1/\xi - (d^2/4\xi_j)]$$

where  $\xi = y + iz$  and subscript refers to  $j$ th vortex. Again, following Nielsen,<sup>10</sup> all the vorticity was concentrated at the vortex cores. At  $x/d = 4$ , average vortex strengths of 2.33 with locations at  $z/d = 0.95$  and  $y/d = \pm 0.35$  were used. At  $x/d = 6$ , vortex strengths of 3.1 were used with  $z/d = 1.15$  and  $y/d = \pm 0.35$ .

Comparisons of the two vortex models with measured crossflow vertical velocity profiles at the  $x/d = 4$  and 6 stations are shown in Figs. 13 and 14. In general, the agreement is extremely good. However, since we know from Fig. 8 that the vorticity is diffuse in the leeside flowfield, we would expect the theory to overpredict the measurements near the vortex cores and to underpredict in the far field. Accordingly, there is then excellent agreement at both stations along the wake axis. At  $x/d = 6$ , the  $z/d = 0.7$  and 1.3 profiles agree, while  $z/d = 1.0$  overestimates and  $z/d = 1.6$  underestimates. At  $x/d = 4$ , the  $z/d = 0.7$  and 1.1 profiles agree, while  $z/d = 0.9$  overestimates and  $z/d = 1.3$  underestimates. Even so, a simple viscous damping would greatly improve the agreement near the vortex cores. But we must also bear in mind that although we have in principle neglected the vortex feeding sheets, in practice we have accounted for some measure of them by contour integration around such large areas of the flowfield. It is possible, therefore, that any contribution we have missed is small compared to the value we have ascribed to the cores.

### Conclusions

It has been shown that, if potential problems associated with directional ambiguity and particle lag are addressed,

meaningful laser velocimeter measurements of high-speed vortex flowfields can be obtained. The present mean flowfield measurements have shown that the vorticity is distributed over large areas of the crossflow plane rather than concentrated near the vortex cores. However, for symmetric vortex flow, satisfactory agreement can still be obtained between the measurements and classical two-dimensional vortex theory, provided the circulation used in the predictions is calculated around contours which account for most of the vorticity in the feeding sheets. Dynamic measurements at the model surface and rms velocity and probability density measurements have shown that vortex unsteadiness may be present in the wake.

### Acknowledgment

This work was supported in part by the Air Force Armament Laboratory, Eglin AFB, Fla., and in part by NASA Ames Research Center, Moffett Field, Calif., under Contract NAS2-9168.

### References

- Thomson, K.D. and Morrison, D.F., "The Spacing, Position and Strength of Vortices in the Wake of Slender Cylindrical Bodies at Large Incidence," *Journal of Fluid Mechanics*, Vol. 50, 1971, pp. 751-783.
- Keener, E.R. and Chapman, G.T., "Onset of Aerodynamic Side Forces at Zero Sideslip on Symmetric Forebodies at High Angles of Attack," AIAA Paper 74-770, Anaheim, Calif., Aug. 1974.
- Lamont, P.J. and Hunt, B.L., "Pressure and Force Distributions on a Sharp-Nosed Circular Cylinder at Large Angles of Inclination to a Uniform Subsonic Stream," *Journal of Fluid Mechanics*, Vol. 76, 1976, pp. 519-559.
- Owen, F.K. and Johnson, D.A., "Measurement of Unsteady Vortex Flowfields," AIAA Paper 78-18, Huntsville, Ala., Jan. 1978.
- Peake, D.J., Owen, F.K., and Higuchi, H., "Symmetrical and Asymmetrical Separations about a Yawed Cone," AGARD CP-247, Oct. 1978.
- Fidler, J.E., Nielsen, J.N., and Schwind, R.G., "An Investigation of Slender-Body Wake Vortices," *AIAA Journal*, Vol. 15, Dec. 1977, pp. 1736-1741.
- Yanta, W.J. and Wardlaw, A.B., "Laser Doppler Velocimeter Measurements of Leeward Flowfields on Slender Bodies at Large Angles of Attack," AIAA Paper 77-660, Albuquerque, New Mexico, June 1977.
- Owen, F.K., "Transition Experiments on a Flat Plate at Subsonic and Supersonic Speeds," *AIAA Journal*, Vol. 8, March 1970, pp. 518-523.
- Morkovin, M.V., 1964 Symposium of Fully Separated Flows, ASME 102, 1964.
- Nielsen, J.N., *Missile Aerodynamics*, McGraw-Hill, New York, 1960, pp. 66-111.

## Make Nominations for an AIAA Award

The following award will be presented during the AIAA Guidance and Control Conference, August 11-13, 1980, Danvers, Mass. If you wish to submit a nomination, please contact Roberta Shapiro, Director, Honors and Awards, AIAA, 1290 Avenue of the Americas, N.Y., N.Y. 10019 (212) 581-4300. The deadline date for submission of nominations is January 3, 1980.

### Mechanics and Control of Flight Award

"For an outstanding recent technical or scientific contribution by an individual in the mechanics, guidance, or control of flight in space or the atmosphere."